World Academy of Science, Engineering and Technology
International Journal of Mechanical and Mechatronics Engineering
Vol:5, No:2, 2011

Bond Graph Modeling of Inter-Actuator Interactions in a Multi-Cylinder Hydraulic System

Mutuku Muvengei and John Kihiu,

Abstract—In this paper, a bond graph dynamic model for a valve-controlled hydraulic cylinder has been developed. A simplified bond graph model of the inter-actuator interactions in a multi-cylinder hydraulic system has also been presented. The overall bond graph model of a valve-controlled hydraulic cylinder was developed by combining the bond graph sub-models of the pump, spool valve and the actuator using junction structures. Causality was then assigned in order to obtain a computational model which could be simulated. The causal bond graph model of the hydraulic cylinder was verified by comparing the open loop state responses to those of an ODE model which had been developed in literature based on the same assumptions. The results were found to correlate very well both in the shape of the curves, magnitude and the response times, thus indicating that the developed model represents the hydraulic dynamics of a valve-controlled cylinder. A simplified model for inter-actuator interaction was presented by connecting an effort source with constant pump pressure to the zero-junction from which the cylinders in a multi-cylinder system are supplied with a constant pressure from the pump. On simulating the state responses of the developed model under different situations of cylinder operations, indicated that such a simple model can be used to predict the inter-actuator interactions.

Keywords—Bond graphs, Inter-actuator interactions, Valve-controlled hydraulic cylinder.

I. Introduction

MOBILE hydraulic systems such as excavators, hydraulic cranes, hydraulic robots, among others, consist of manipulator joints which are powered by hydraulic cylinders. More than one cylinders are consequently powered by one hydraulic pump.

Among the characteristics which must be captured by the dynamic model of a mobile hydro-mechanical system with an articulated arm are the actuator interactions which are important since they significantly affect the overall response of the system [1]. The interaction between the different actuators occurs due to the fact that they are powered by a single power engine. When multiple actuators request flow simultaneously, the power demand may exceed the capacity of the engine. The hydraulic system is forced to reduce the flow to the cylinders to keep the engine from stalling. Therefore the actuator interaction is an important part of system dynamics and must be modeled.

Singh et al. [2] used a simple approach to handle the flow distribution between multiple hydraulic actuators. The authors assumed a fixed pump flow (even though pumps vary their output), and assumed that the circuit with a valve closest to the pump gets all the flow it requires, and that the remaining flow is distributed among the rest. This approach is valid when the cylinders have similar force loads, but not when the cylinders have very different force loads. There is no literature available on how to model the flow distribution of multiple cylinders without resorting to detailed model. This research work addresses this shortcoming.

The relatively new bond graph modeling technique, has been proposed to successfully model the interaction of power between elements on a system. Bond graphs model the power flow in a system and the state equations are formulated directly from this graphical representation. As this paper demonstrates, bond graphs can quickly and accurately model and simulate the dynamics in a hydraulic system, including the dynamic interaction of the actuators involved.

Once the bond graph model is ready, the system equations can be derived from it algorithmically in a systematic manner. This process is usually automated using appropriate softwares such as ENPORT, CAMP-G, TUTSIM 20-SIM, SYMBOLS 2000, etc which support bond graphs.

The concept of bond graphs was originated by Paynter [3]. The idea was further developed by Karnopp and Rosenberg in their textbooks [4]–[6], such that it could be used in practice. By means of the formulation by Breedveld [7] of a framework based on thermodynamics, bond graph model description evolved to a systems theory. More information about bond graphs can be found in [4]–[10].

In this paper, the hydraulic dynamics of a valve-controlled hydraulic cylinder is developed and validated, and then a simplified model of inter-actuator interactions on a multi-cylinder hydraulic system is presented. The models are derived from first principles in order to contribute to educational material regarding the bond graph modeling tool.

II. Modeling the Dynamics of a Double Acting Valve-Controlled Hydraulic Cylinder

A. Bond Graph model Development

The hydraulic dynamics to be modeled are the actuator dynamics, which herein refer to the dynamics of the hydraulic pump, spool valves and the hydraulic actuator as shown in Fig. 1.

The following is a summary of the assumptions that were made when developing the bond graph dynamic model of a valve-controlled hydraulic cylinder;

Mr. M. Muvengei, Department of Mechanical Engineering, Jomo Kenyatta University of Agriculture and Technology, P.O BOX 62000-00200 Kenya (Tel: +254720642441, e-mail: mmuvengei@eng.jkuat.ac.ke.)
Prof. Eng. J. Kihiu, Department of Mechanical Engineering, Jomo Kenyatta University of Agriculture and Technology, P.O BOX 62000-00200 Kenya (email: kihiusan@yahoo.com)

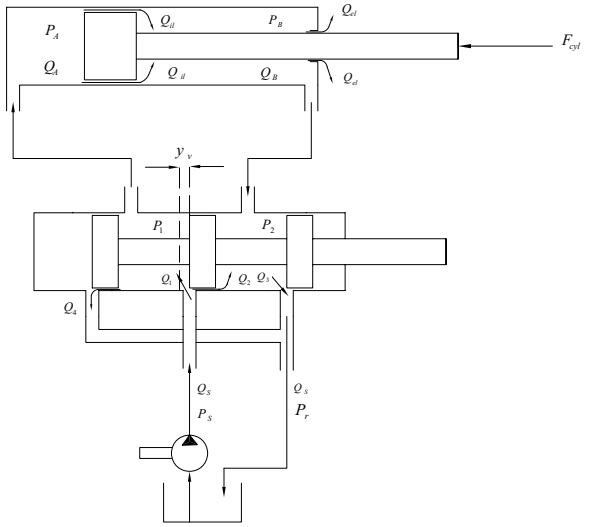

Fig. 1. Schematic diagram of a valve controlled hydraulic cylinder.

- The hydraulic pump delivers a constant supply pressure, irrespective of the oil flow demand. This implies that P_S is constant.
- The reservoir (tank) pressure is constant and at atmospheric pressure. Since gauge pressures are considered then $P_r = 0$.
- The flows through the valves are turbulent.
- The leakage flow through the clearance between the cylinder and the piston is laminar.
- Possible dynamical behavior of the pressure in the transmission lines between valves and actuators are assumed to be negligible. This means that $P_A = P_1$, and $P_B = P_2$.
- The spool valve is matched and symmetrical. Its bandwith is much higher than the band-width of the cylinder, so that the valve dynamics due to inertia can be neglected. [11]
- External leakage Q_{el} between the piston rod and the external seals is neglected. This is because external leakage on the cylinder must be avoided by use of improved sealing technology.
- Inefficient volumes, i.e., the volume of the fluid in the hoses between the valve and the actuator, and the volume of oil existing in the cylinder, are neglected.
- The cylinder chambers are assumed to be rigid, i.e., no compliance in the walls. The stiffness of the cylinder chambers is more than five times higher than that of the hydraulic oil. Therefore when operating at the same pressure range, the compliance effect from cylinder walls is negligible compared to the oil compliance.
- Viscous friction effects in the piston seals are assumed to be dominant compared to the coulomb friction effects. Hydraulic oil lubricates the sliding passages in the cylinder and this greatly reduces the effects of coulomb friction.

B. Pump

The pump is assumed to be an ideal source of power capable of supplying constant pressure at any flow required. An ideal power source is capable of supplying constant pressure at any flow required. Real pressure sources on the other hand, have limits on the power that they can supply. In practical hydraulic pump analysis, leakage flows and friction are counted as sources of power loss in pumps. Although this is certainly true in reality, hydraulic machines are quite efficient. For piston pumps, their efficiencies are always around 90% within the normal operating range. Therefore the pump is assumed to be an ideal source of power and can be modeled in bond graph form as an effort source, as shown in Fig. 2.

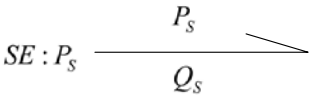

Fig. 2. Constant pressure pump bond graph model

C. Spool Valves

One of the criteria in selecting valves is to consider their response time. If the resonant frequency of the spool valve is very high, its dynamic behavior is negligible compared to the relatively low resonant frequency of the system [12]. A typical industrial manipulator has a natural frequency in the range of $1-5Hz$, while the cut-off frequency of the selected valves when operating under maximum command must be in the range of $10-15Hz$ [13]. Thus only the resistive effect of the valve is considered.

To model the dynamics of the spool valve due to its resistive effect to the fluid flow, the following two assumptions are made for analysis;

- The hydraulic fluid is ideal, non-viscous and incompressible. This assumption is close to reality under most conditions and is also justified as far as phenomena inside the valve are considered.
- Valve geometry is ideal. This implies that the edges of the metering orifices are sharp and that the working clearances are zero, hence no-internal leakage condition is assumed [14]–[16].

The orifice flow equation governing flow and pressure drop across an orifice (for turbulent flow) is known to be [15],

$$Q = C_d A_O \sqrt{\frac{2}{\rho}\Delta P} \tag{1}$$

Where;

- Q is the flow rate through the orifice,
- ΔP is the pressure drop across the orifice,
- C_d is the discharge coefficient,
- ρ is the fluid density,
- A_O is the area of the orifice opening.

Equation 1 shows that the relative flow rates are dependent on the pressure drops across the valves, which in turn are dependent on the forces acting on the actuator.

Let the spool be given a positive displacement from the neutral position, i.e, $y_v = 0$ which is chosen to be the symmetrical position of the spool in its sleeve. Using 1, the flow rates through the metering orifices are,

$$Q_1 = C_d A_{O1}\sqrt{\frac{2}{\rho}(P_S - P_1)} \tag{2}$$

$$Q_2 = C_d A_{O2}\sqrt{\frac{2}{\rho}(P_S - P_2)} \tag{3}$$

$$Q_3 = C_d A_{O3}\sqrt{\frac{2}{\rho}(P_2 - P_r)} \tag{4}$$

and

$$Q_4 = C_d A_{O4}\sqrt{\frac{2}{\rho}(P_1 - P_r)} \tag{5}$$

The return pressure $P_r = 0$, since the tank pressure is taken to be at atmospheric. Since the geometry of the valve is assumed ideal and the valving orifices are matched and symmetrical then $Q_2 = Q_4 = 0$, and $A_{O1} = A_{O3} = A_O(y_v)$.

Note that from Fig. 1, the total supply flow (Q_S) is given as;

$$Q_S = Q_1 + Q_2 = Q_1 \tag{6}$$

and also as;

$$Q_S = Q_3 + Q_4 = Q_3 \tag{7}$$

From Fig. 1, flow to the chamber A of cylinder and flow out of chamber B of the cylinder are given as;

$$\begin{aligned} Q_A &= Q_1 - Q_4 \\ &= Q_1 \\ &= C_d A_O(y_v)\sqrt{\frac{2}{\rho}(P_s - P_A)} \end{aligned} \tag{8}$$

and

$$\begin{aligned} Q_B &= Q_3 - Q_2 \\ &= Q_3 \\ &= C_d A_O(y_v)\sqrt{\frac{2}{\rho}(P_B - P_r)} \end{aligned} \tag{9}$$

The area of the valve orifice opening is dependent on the valve spool displacement (y_v) as shown in Fig. 3.

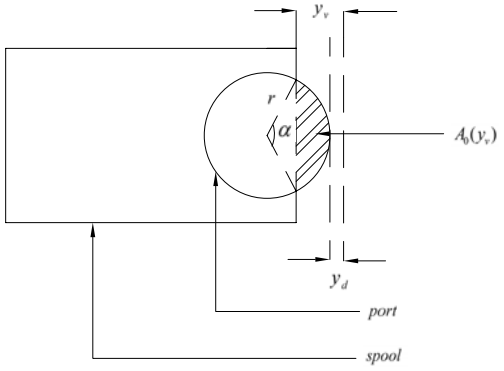

Fig. 3. Variation of valve orifice area with spool movement

If the port is of radius r, the uncovered area of the orifice where the fluid passes is given,

$$\begin{aligned} A_O(y_v) &= \frac{\alpha}{2\pi}\pi r^2 - \frac{1}{2}(2r\sin\frac{\alpha}{2})r\cos\frac{\alpha}{2} \\ &= \frac{r^2}{2}(\alpha - \sin\alpha) \end{aligned} \tag{10}$$

Where α varies with the valve displacement as shown below;

$$\begin{aligned} \cos\frac{\alpha}{2} &= \frac{r - (y_v - y_d)}{r} \\ \alpha &= 2\cos^{-1}\Big(\frac{r - (y_v - y_d)}{r}\Big) \end{aligned} \tag{11}$$

Equations 8 and 9 show that the flow that is transferred from the pump to the cylinder is determined by the flow coefficient, the area of the valve orifice and the pressure difference. These equations are appropriate expressions for the constitutive relations of orifice resistances to the flow rate to and from the cylinder and can be represented as;

$$P_s - P_A = \Delta P_A = \frac{\rho}{2C_d^2(A_O(y_v))^2}Q_A|Q_A| = R_1 Q_A|Q_A| \tag{12}$$

and

$$P_B - P_r = \Delta P_B = \frac{\rho}{2C_d^2(A_O(y_v))^2}Q_B|Q_B| = R_2 Q_B|Q_B| \tag{13}$$

The absolute value sign has been used to correct the sign in the pressure drop for negative flow rate.

Equations 12 and 13 show that the valve resistances are equal, i.e.,

$$R_1 = R_2 = \frac{\rho}{2C_d^2(A_O(y_v))^2} \tag{14}$$

Hence the valve resistances R_1 and R_2 given in 14 depend on the position of the valve (y_v). The bond graph representation of the valve resistance effects to the fluid flow to and from the cylinder are shown in Figs. 4 and 5.

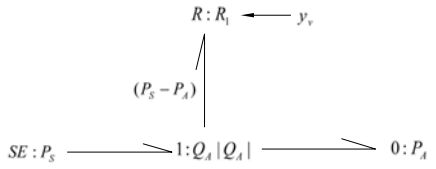

Fig. 4. Bond graph representation of valve resistance to forward flow

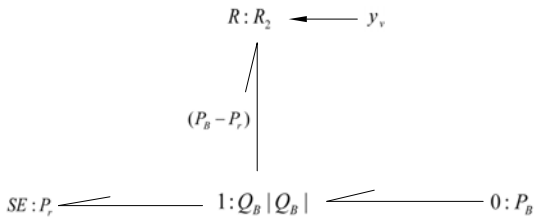

Fig. 5. Bond graph representation of valve resistance to return flow

An active bond has been used to indicate that the valve resistances depend on the valve displacements. An active bond

is just like a signal in a block diagram, and is shown with a full arrow. The active bond implies that no feedback effect is considered, i.e., an effort or flow signal is transmitted in one direction, the complimentary signal does not flow in the opposite direction as in a normal bond [6].

D. Linear Cylinders

Figure 6 shows a schematic diagram of a hydraulic cylinder. The cylinder piston has diameter D_p, area A_p and the rod has diameter D_r and area A_r.

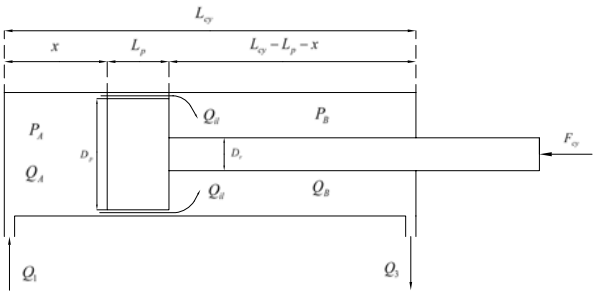

Fig. 6. Schematic diagram of the linear actuator

The chamber at the head side has a pressure P_A and flow rate Q_A, and are positive into the cylinder. The chamber at the rod side has pressure P_B and flow rate Q_B, and are positive out of the cylinder.

Hydraulic cylinders transform hydraulic energy into mechanical energy, i.e., the pressure difference at the two cylinder chambers provide mechanical force which drives the piston. Bond graph method identifies this transformation in terms of transformer elements, which can be represented as shown in Fig. 7.

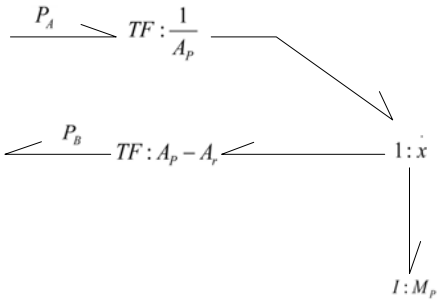

Fig. 7. Bond graph representation of the pressure difference in cylinder chambers

The piston and rod mass of the cylinder, is modeled as a $I-$element which is attached to the $1-$junction with the piston velocity $(\dot{x})$ as the common variable.

1) Modeling Oil Compressibility in a Hydraulic Cylinder: The influence of the finite oil stiffness on the dynamics of hydraulic system is similar to that of a spring compressibility in mechanical systems. A measure of oil compressibility is the bulk modulus, which relates the variation of pressure and volume of oil in a closed vessel as shown below [15],

$$\Delta p = \beta\Big(\frac{-\Delta V}{V}\Big) \tag{15}$$

where

- β is the Bulk Modulus of the fluid
- ΔV is the decrease in volume of the fluid due to pressure
- V is the volume itself.

Equation 15 is usually considered the constitutive law of a linear one port $C-$element of compliance $C = \frac{V}{\beta}$, attached to the zero junction representing the hydrostatic pressure [17], as shown in Fig. 8.

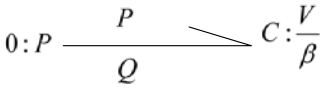

Fig. 8. C-element representing fluid compressibility

Application of 15 to the chambers of a hydraulic cylinder however reveals a problem with respect to a correct bond graph representation, since the chamber volume depends on the displacement x of the piston. Therefore,

$$\Delta p = \beta\frac{-\Delta V}{V_o + A_p x_p} \tag{16}$$

where

- V_o is the volume of chamber at start position $x = x_o$
- A_p is the area of the piston.

The compliance $\frac{V_o+A_p x}{\beta}$ can be considered as a displacement dependent compliance $(C(x))$, i.e.,

$$C(x) = \frac{V_o + A_p x}{\beta} \tag{17}$$

Equation 17 can be depicted in the bond graph by means of a modulation signal as shown in Fig. 9.

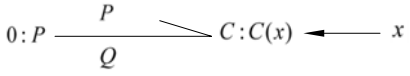

Fig. 9. Displacement Modulated C element

The displacement dependent compliance in 17 has been taken into account without expressing the modulation in the bond graph [18], but this means that the bond graph does not properly correspond to the mathematical model in use.

Each chamber therefore has displacement dependent compliance C_A and C_B given as;

$$C_A = \frac{V_A}{\beta} = \frac{A_p x}{\beta} \tag{18}$$

and

$$C_B = \frac{V_B}{\beta} = \frac{(A_p - A_r)(L_{cy} - L_p - x)}{\beta} \tag{19}$$

Equations 18 and 19 can be represented in bond graph form as in Figs. 10 and 11,

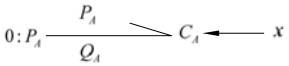

Fig. 10. Displacement Modulated C element of cylinder chamber A

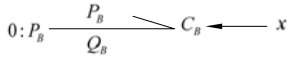

Fig. 11. Displacement Modulated C element of cylinder chamber B

2) Modeling the Leakage Flows: There is always some clearance between the cylinder and the piston to allow relative motion. Even though these clearances are small in comparison with the normal cross-sectional area of the oil flow in a circuit, they act as leakage paths when pressure drops are imposed [11]. Internal leakage occurs in hydraulic cylinders as result of a pressure difference existing between the two chamber.

The fluid flow rate in the clearance can be obtained from Hagen-Poisseille equation as;

$$Q_{il} = \frac{\pi D_p c^3}{12\mu L_p}(P_A - P_B) \tag{20}$$

where c and μ are the radial clearance between the piston and the cylinder wall, and the coefficient viscosity of the hydraulic fluid respectively.

Equation 20 can be depicted in bond graph form as shown in Fig. 12.

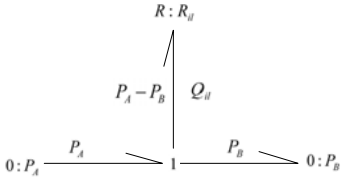

Fig. 12. Bond graph model representing the leakage in piston and cylinder wall clearance

Where

$$R_{il} = \frac{12\mu L_p}{\pi D_p c^3} \tag{21}$$

3) Modeling the Viscous Friction: Another object in developing a correct bond graph model of a double acting hydraulic cylinder is the viscous friction which generally oppose the piston movements. This viscous friction has been considered by few authors, e.g. in [17], [19], often it is simply neglected.

Viscous friction due to piston movement is described by Newton's law as [15],

$$F_N = \mu \frac{A}{c}\frac{\partial x}{\partial t} = \mu \frac{\pi D_p L_p}{c}\dot{x} \tag{22}$$

This viscous friction due to the piston movement is modeled as a $R-$element attached to the $1-$junction with the piston velocity $(\dot{x})$ as the common variable. This is shown in Fig. 13,

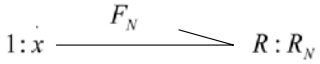

Fig. 13. Bond graph model representing the viscous friction due to piston movement

Where

$$R_N = \frac{\mu \pi D_p L_p}{c} \tag{23}$$

E. Overall Bond Graph Model of a Valve Controlled Double Acting Cylinder

Figure 14 shows the overall bond graph model of a valve-controlled hydraulic cylinder with causality assigned using Sequential Causality Assignment Procedure (SCAP) as clearly illustrated in [7], [8], [10]. The bonds are numbered for easier analysis purposes.

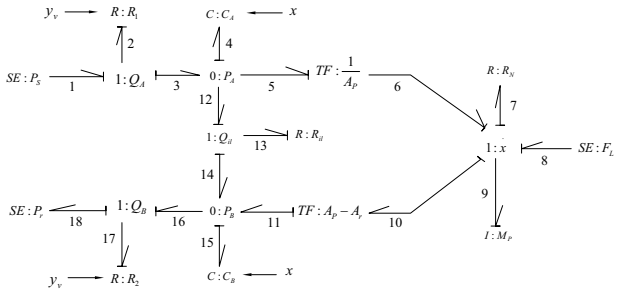

Fig. 14. A causal bond graph model for the cylinder during extension.

Next is to check if the bond graph model developed embodies the basic laws of mass continuity (continuity equation) and the equation of motion for mechanical moving parts (Newton's second law).

The continuity equation [15] can be represented as;

$$\sum Q_{in} - \sum Q_{out} = \frac{dV}{dt} + \frac{V}{\beta}\frac{dP}{dt} \tag{24}$$

Where

- $\sum Q_{in}$ is the total input flows of the fluid
- $\sum Q_{out}$ is the total output flows of the fluid
- V is the volume of the fluid subjected to compression
- $\frac{dV}{dt}$ is the flow consumed by the expansion of control volume
- $\frac{V}{\beta}\frac{dP}{dt}$ is the compressibility flow and describes the flow resulting from pressure changes.

From the bond graph model of the cylinder shown in Fig. 14

$$\begin{aligned}
e_3 &= e_4 = e_5 = e_{12} = P_A \\
e_4 &= \frac{1}{C_A}\int f_4 dt \\
f_4 &= \frac{A_p x}{\beta}\left(\frac{dP_A}{dt}\right) \\
f_1 &= f_2 = f_3 = Q_1 = C_d A_O(y_v)\sqrt{\frac{2}{\rho}(P_S - P_A)} \\
f_6 &= f_7 = f_8 = f_9 = f_{10} = \dot{x} \\
f_5 &= \frac{1}{r_1}\dot{x} = A_p\dot{x} \\
e_6 &= \frac{1}{r_1}e_5 = A_p P_A \\
e_7 &= R_N f_7 = \frac{\mu\pi D_p L_p}{c}\dot{x} \\
e_8 &= F_L \\
e_9 &= M_p\dot{f}_9 = M_p\ddot{x} \\
e_{11} &= e_{14} = e_{15} = e_{16} = P_B \\
e_{15} &= \frac{1}{C_B}\int f_{15} dt
\end{aligned}$$

$$
\begin{aligned}
f_{15} &= \frac{(A_p - A_r)(L_{cy} - L_p - x)}{\beta}\Big(\frac{dP_B}{dt}\Big)\\
e_{10} &= r_2 e_{11} = (A_p - A_r)P_B\\
f_{11} &= r_2\dot{x} = (A_p - A_r)\dot{x}\\
f_{16} &= f_{17} = f_{18} = Q_3 = C_d A_O(y_v)\sqrt{\frac{2}{\rho}P_B}\\
e_{13} &= e_{12} - e_{14} = P_A - P_B\\
f_{12} &= f_{13} = f_{14} = \frac{1}{R_{HP}}e_{13} = \frac{\pi D_p c^3}{12\mu L_p}(P_A - P_B)
\end{aligned}
$$

Summing the flow variables in the 0-junction with common head side pressure (P_A), we get;

$$f_3 = f_4 + f_5 + f_{12}$$

$$
\begin{aligned}
C_d A_O(y_v)\sqrt{\frac{2}{\rho}(P_S - P_A)} = \frac{A_p x}{\beta}\Big(\frac{dP_A}{dt}\Big) + A_p\dot{x}\\
+\frac{\pi D_p c^3}{12\mu L_p}(P_A - P_B)
\end{aligned}
$$

$$
\begin{aligned}
A_p\dot{x} + \frac{A_p x}{\beta}\Big(\frac{dP_A}{dt}\Big) = C_d A_O(y_v)\sqrt{\frac{2}{\rho}(P_S - P_A)}\\
-\frac{\pi D_p c^3}{12\mu L_p}(P_A - P_B) \qquad (25)
\end{aligned}
$$

Equation 25 shows that the continuity equation at the head side of the cylinder is satisfied.

Summing the flow variables in the 0-junction with common rod side pressure (P_B), we get;

$$f_{11} + f_{14} = f_{15} + f_{16}$$

$$
\begin{aligned}
(A_p - A_r)\dot{x} + \frac{\pi D_p c^3}{12\mu L_p}(P_A - P_B) = C_d A_O(y_v)\sqrt{\frac{2}{\rho}P_B} +\\
\frac{(A_p - A_r)(L_{cy} - L_p - x)}{\beta}\Big(\frac{dP_B}{dt}\Big)
\end{aligned}
$$

$$
\begin{aligned}
-(A_p - A_r)\dot{x} + \frac{(A_p - A_r)(L_{cy} - L_p - x)}{\beta}\Big(\frac{dP_B}{dt}\Big) =\\
\frac{\pi D_p c^3}{12\mu L_p}(P_A - P_B) - C_d A_O(y_v)\sqrt{\frac{2}{\rho}P_B} \qquad (26)
\end{aligned}
$$

Equation 26 above shows that the continuity equation at the rod side of the cylinder is satisfied.

Summing the effort variables in the 1-junction with common piston velocity, we get;

$$e_9 + e_{10} + e_7 = e_8 + e_6$$

Therefore,

$$
\begin{aligned}
e_9 &= e_6 - e_{10} - e_7 + e_8\\
M_p\ddot{x} &= A_p P_A - (A_p - A_r)P_B - \frac{\mu\pi D_p L_p}{c}\dot{x} - F_L \qquad (27)
\end{aligned}
$$

Equation 27 shows that the Newton's second law of motion is satisfied.

F. Checking the Bond Graph model

The bond graph model of the hydraulic dynamics of the actuator was validated by comparing the open loop state responses of the cylinder obtained from simulating the bond graph model, to those obtained by simulating the Ordinary Differential Equation (ODE) model of a cylinder developed by Nguyen [11] based on the same assumptions. The parameters of the arm cylinder as shown in table I, together with hydraulic parameters in table II were used in simulating the two models.

To simulate the state responses of the hydraulic cylinder from bond graph model, the causal bond graph model of the hydraulic cylinder shown in Fig. 14 under no load $F_L = 0$, was first converted into block diagram using the Fakri method [9]. The block diagram representing the bond graph was then simulated on SIMULINK to obtain the state responses of the hydraulic cylinder on extension/retraction and under no load.

The ODE model of a hydraulic cylinder developed by [11] based on first principles of the basic laws of mass continuity (continuity equation) and the equation of motion for mechanical moving parts (Newton's second law), has the following state space representation;

$$\dot{y_1} = y_2 \qquad (28)$$

$$\dot{y_2} = \frac{1}{M_p}\Big[y_3 A_p - y_4(A_p - A_r) - \frac{\mu\pi D_p L_p}{c}y_2 - F_L\Big] \qquad (29)$$

$$
\begin{aligned}
\dot{y_3} = \frac{\beta}{A_p y_1}\Big[C_d A_O(y_v)\sqrt{\frac{2}{\rho}(P_S - y_3)} - A_p y_2 - C_{ip}\\
(y_3 - y_4)\Big] \qquad (30)
\end{aligned}
$$

$$
\begin{aligned}
\dot{y_4} = \frac{\beta}{(A_p - A_r)(L_{cy} - L_p - y_1)}\Big[-C_d A_O(y_v)\sqrt{\frac{2}{\rho}y_4}\\
+(A_p - A_r)y_2 - C_{ip}(y_3 - y_4)\Big] \qquad (31)
\end{aligned}
$$

where a state vector was defined as;

$$\begin{pmatrix} y_1\\ y_2\\ y_3\\ y_4 \end{pmatrix} = \begin{pmatrix} x\\ \dot{x}\\ P_A\\ P_B \end{pmatrix} \qquad (32)$$

Equations 28 to 31 can be solved using MATLAB ODE-solvers, and then the state responses simulated. The open loop state responses of the cylinder on extension and retraction are shown in Figs. 15, and 16 respectively.

The results are seen to correlate very well both in the shape of the curves, magnitude and the response times, thus indicating that the developed model represents the hydraulic dynamics of a valve controlled cylinder

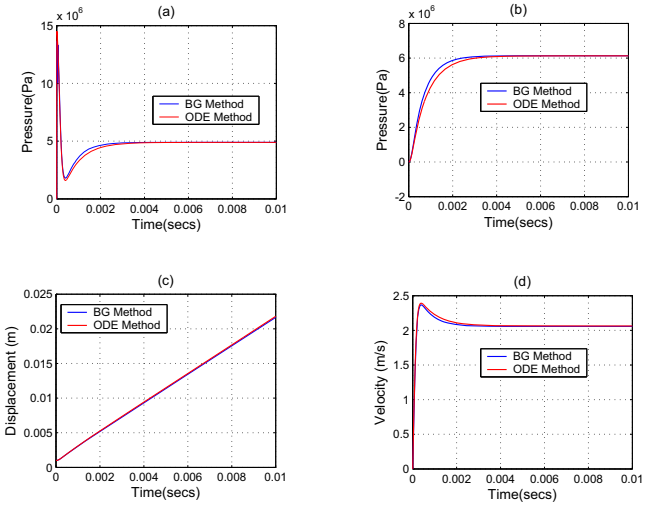

Fig. 15. Simulated open loop responses of the cylinder for extension case; **(a)** Head side chamber pressure **(b)** Rod side chamber pressure **(c)** Piston displacement **(d)** Piston velocity

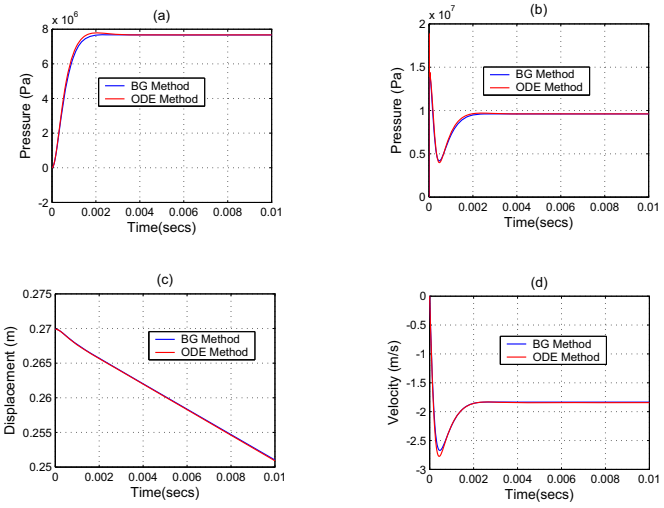

Fig. 16. Simulated open loop responses of the cylinder for retraction case; **(a)** Head side chamber pressure **(b)** Rod side chamber pressure **(c)** Piston displacement **(d)** Piston velocity

III. Inter-Actuator Interaction

Among the characteristics which must be captured by the dynamic model of a mobile hydro-mechanical system with an articulated arm, such as excavators, hydraulic cranes, hydraulic robots, among others, are the actuator interactions which are important since they significantly affect the overall response of the system

Since the pump was modeled as a constant pressure supply, the it supplies a constant pressure to all cylinders connected to it regardless of the flow demand across each actuator. Therefore an Effort Source with constant pressure as the source (that is, $SE : P_S$), is connected to the zero junction from which the cylinders are supplied with constant pressure.

To demonstrate the inter-actuator interaction, two cylinders being driven by one hydraulic pump as shown in Fig. 17 were considered.

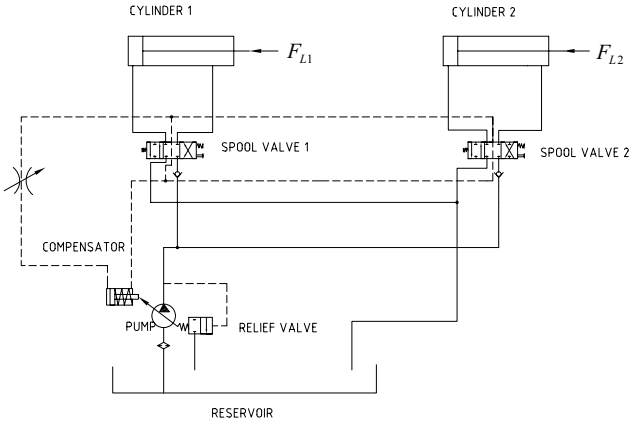

Fig. 17. Hydraulic circuit for two cylinders powered by one pump.

The bond graph model representing the actuators is shown in Fig. 18.

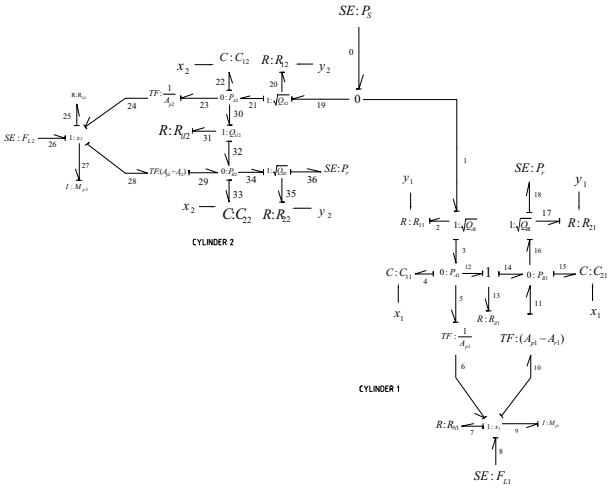

Fig. 18. Bond graph models of two hydraulic cylinders powered by one pump.

Using the parameters of the boom and arm cylinders as given in table I together with hydraulic parameters in table II, the open loop responses of the hydraulic actuators under step inputs were simulated for four cases, that is,

- *Case 1:* When the two cylinders are moving no load and their directional control valves are equally displaced.
- *Case 2:* When the two cylinders are moving no load and one directional control valve, i.e., for cylinder 1 is closed.
- *Case 3:*When the cylinders are moving no load and the step inputs to the cylinders are different.
- *Case 4:* When the two cylinders are moving different loads.

Four open loop state responses of the cylinders, that is, chamber pressures, fluid flow rates, piston velocities, and piston displacements (the integral of piston velocities), were simulated to show how the dynamics of the two cylinders interacted during the hydraulic system performance under the above conditions.

Case 1

In this case the two cylinders were given equal step inputs equivalent to the maximum spool valve displacements, and their open loop responses simulated when the cylinders were assumed to move no load. Figure 19 shows the responses for case 1.

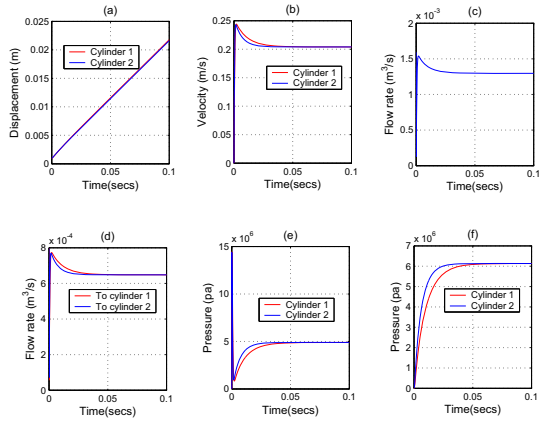

Fig. 19. Simulated open loop responses for case 1; **(a)** Piston displacements **(b)** Piston velocities **(c)** Pump flow rate **(d)** Flow rate to cylinders **(e)** Head sides chamber pressures **(f)** Rod side chamber pressures

As seen in Fig. 19, the only difference between the response curves of the two cylinders is the speed of response. Cylinder 2 which has a smaller piston and rod mass, has a fast response compared to cylinder 1 which has a relatively larger piston and rod mass. This is what is expected practically since a body with a large mass has a consequent large inertia which slows down the response speed to movements.

Case 2

In this case, the spool valve controlling cylinder 1 remained closed while cylinder 2 was given a step input equivalent to the maximum spool valve displacement. Also the two cylinders were assumed to move no load. Figure 20 shows the responses for case 2.

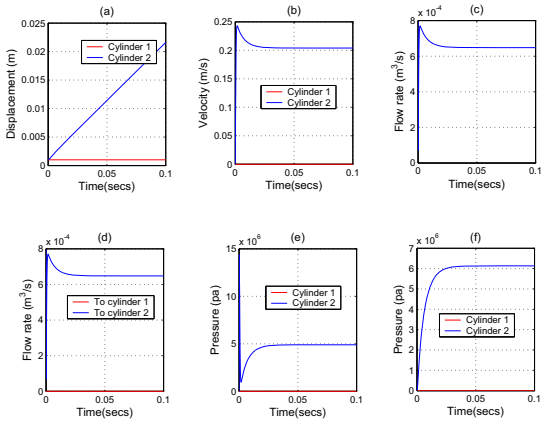

Fig. 20. Simulated open loop responses for case 2; **(a)** Piston displacements **(b)** Piston velocities **(c)** Pump flow rate **(d)** Flow rate to cylinders **(e)** Head sides chamber pressures **(f)** Rod side chamber pressures

As seen in Fig. 20**(d)**, there is no fluid flow to cylinder 1 since the spool valve controlling this cylinder is closed. Due to this, there is no hydraulic pressures generated in cylinder 1 chambers as shown in Figs. 20**(e)** and **(f)**, and subsequently the piston of cylinder 1 remains stationary as illustrated in Figs. 20**(a)** and **(b)**. The pump produces only the flow required to operate cylinder 2. This flow creates a pressure drop across cylinder 1 which moves the piston of the cylinder. This is what is expected practically, since a hydraulic cylinder whose spool valve is completely closed, has no flow into it and subsequently no motion results, hence no response.

Case 3

In this case, cylinder 2 was given a step input equivalent to the maximum spool displacement, while cylinder 1 was given a step input equivalent to half of the maximum spool displacement. This implies that, the spool valve controlling cylinder 2 had a wider orifice opening than the one controlling cylinder 1. Figure 21 shows the responses for case 3.

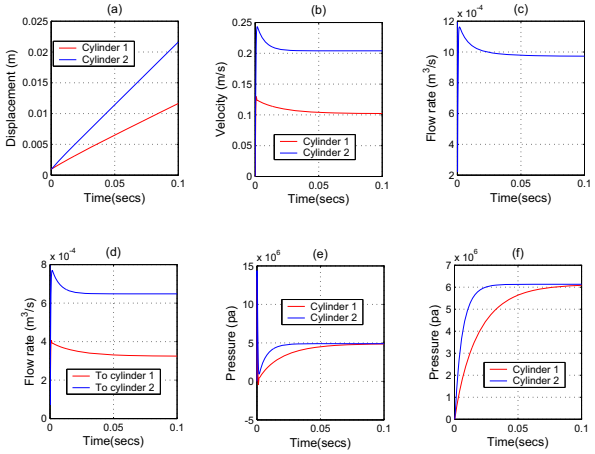

Fig. 21. Simulated open loop responses for case 3; **(a)** Piston displacements **(b)** Piston velocities **(c)** Pump flow rate **(d)** Flow rate to cylinders **(e)** Head sides chamber pressures **(f)** Rod side chamber pressures

As seen in Fig. 21**(d)**, cylinder 2 whose directional control valve has a wider orifice opening area receives much fluid flow from the pump as compared to cylinder 1. This is because the larger the area of the orifice, the smaller the valve resistance to fluid flow, and since the flow rate through the valve is inversely proportional to the valve resistance as evident in 12, then it follows that, flow rate through the valve is higher for large orifice openings. This larger flow to cylinder 2 results in faster pressure accumulation in the cylinder chambers as shown in Figs. 21**(e)** and **(f)**, and this subsequently leads to high piston speeds as evident in Fig. 21**(b)**.

Case 4

In this case, both cylinders were given similar step inputs equivalent to maximum spool displacements, while the cylinder rods moved different external and translational loads. Figure 22 shows the responses for case 4.

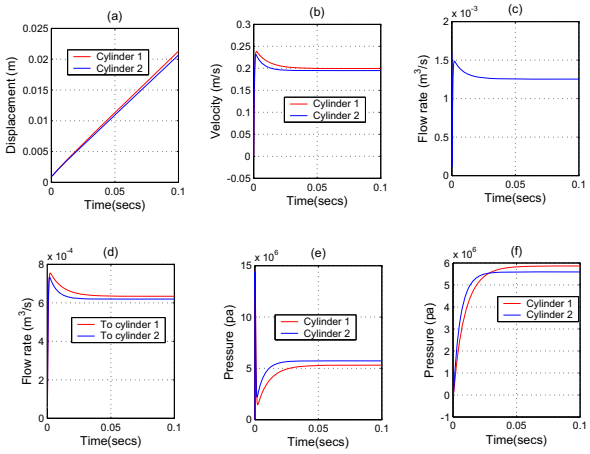

Fig. 22. Simulated open loop responses for case 4; **(a)** Piston displacements **(b)** Piston velocities **(c)** Pump flow rate **(d)** Flow rate to cylinders **(e)** Head sides chamber pressures **(f)** Rod side chamber pressures

Cylinder 1 moves half of the force moved by cylinder 2. A large pressure drop is required by cylinder 2 so as to produce a force big enough to move the large external load. This large pressure drop for cylinder 2 is evident in Figs. 22**(e)** and **(f)** as compared to a relatively smaller pressure drop required to move a lighter load by cylinder 1. Since the external force to be moved offers a resistance to fluid flow to the actuators, then it follows that the larger the load to be moved, the smaller the fluid flow to the cylinder. This is the reason why fluid flow to cylinder 2 is relatively small compared to the flow to cylinder 1 as shown in Fig. 22**(d)**. This difference in fluid flow rates to the cylinders results to different cylinder piston speeds as shown in Fig. 22**(b)** with a large piston velocity produced by the cylinder moving the smaller load.

IV. Conclusion

In this paper, a detailed model of a valve-controlled hydraulic cylinder has been quickly and accurately developed using the relatively new bond graph modeling tool. The model was developed from first principles, and hence this work can be used as an educational tool on bond graphs.

Further, it was shown that, representing the multi-cylinder hydraulic system bond graph models as shown in Fig. 18, can predict what is practically expected regarding the inter-actuator interaction in a simplified way. Although such representation is expected to give an error in state responses of the overall hydraulic and mechanical dynamic model of a mobile hydro-mechanical system, since for several cylinders operating simultaneously, each one of them has its own requirement for supply pressure depending on the load and speed required from it, but for simplicity it was assumed that the supply pressure for all the cylinders are equal and constant.

Appendix A
Hydraulic Cylinder Parameters

Table I shows the hydraulic cylinders parameters used in simulations.

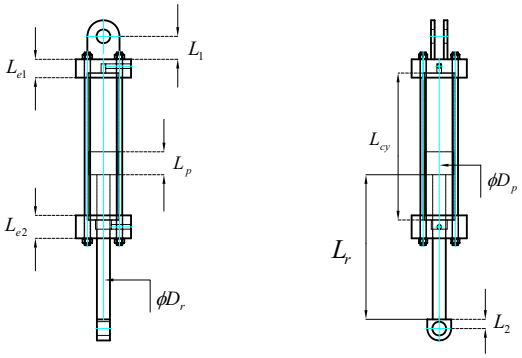

Fig. 23. Schematic diagram of hydraulic cylinders.

TABLE I
Hydraulic Cylinder Parameters.

Parameter description		Units	Boom	Arm	Bucket
Length of cylinder barrel	L_{cy}	*mm*	480	320	395
Length of rod,	L_r	*mm*	450	290	365
Length of stroke,	L_s	*mm*	430	270	345
Length of piston,	L_p	*mm*	50	50	50
Diameter of piston,	D_p	*mm*	63.5	63.5	63.5
Diameter of rod,	D_r	*mm*	28.5	28.5	28.5
Length of end cap1 ,	L_{e1}	*mm*	30	30	30
Length of end cap2,	L_{e2}	*mm*	40	40	40
Length of bracket1,	L_1	*mm*	50	50	50
Length of bracket2,	L_2	*mm*	20	20	20

Appendix B
Pump, Valve and Hydraulic Fluid Parameters

Table II shows the pump, valve and hydraulic fluid parameters used in simulations.

TABLE II
Pump, Valve and Hydraulic Parameters.

Pump parameters		
Maximum operating pressure (P_{max})	17.0×10^6	*Pa*
Maximum flow rate (Q_{max})	65	*lit* / min
Maximum speed (N_{max})	2500	*rpm*
Supply pressure (P_s)	14.5×10^6	*Pa*
Directional control valve parameters		
Discharge coefficient (C_d)	0.61	
Diameter of ports (d)	9.525	*mm*
Maximum flow rate (Q_{max})	40	*lit* / min
Maximum operating pressure (P_{max})	35.0×10^6	*Pa*
Hydraulic fluid parameters		
Bulk mudulus (β)	1.6×10^9	*Pa*
Fluid density (ρ)	850	Kg/m^3
Fluid absolute viscosity (μ) at 25^0C	7.9×10^{-4}	m^2/s

References

[1] M. Krishna, *"Optimal Motion Generation for Hydraulic Robots"*. PhD. thesis, 1999.
[2] N. Singh, "Coordinated motion control of heavy duty industrial machines with redundancy," *Journal of Robotica*, vol. 13, pp. 623–633, 1995.
[3] H. M. Paynter, *Analysis and Design of Engineering Systems*. MIT Press Publishers, Cambridge, 1961.

[4] D. C. Karnopp, D. L Margolis, and R. C. Rosenberg, *System Dynamics: Modelling and Simulation of Mechatronic Systems*. John Wiley and Sons Publishers, Newyork, 2000.
[5] D. C. Karnopp, D. L. Margolis, and R. C. Rosenberg, *System Dynamics; A Unified Approach*. John Wiley and Sons Publishers, Newyork, 2nd ed., 1990.
[6] D .C. Karnopp and R. C. Rosenberg, *Introduction to Physical System Dynamics*. McGraw Hill Publishers, Newyork, 1983.
[7] P. Breedveld, "Bond graphs," in *Encyclopedia of Life Support Systems, Modeling and Simulation*, 2003.
[8] P. Gawthrop and L. Smith, *Metamodeling: Bond Graphs and Dynamic Systems*. Prentice Hall International Publishers, UK Limited, 1996.
[9] F. Fakri, A. Rocaries, and A. Carrierre, "A simple method for conversion of bond graph models in representation by block diagrams," in *1997 Proc. International Conference on Bond Graph Modeling and Simulation*.
[10] J. F. Broenink, "Introduction to Physical Systems Modeling with Bond Graphs," Technical Report, Department of Electrical Engineering, University of Twente, Netherlands, 1996.
[11] H. Q. Nguyen, *"Robust low level control of robotic excavation"*. PhD. thesis, Australian Centre for Field Robotics, The University of Sydney, 2000.
[12] M. Bin, "System modeling, identification and coordinated control design for an articulated forestry machine," MSc. thesis, Department of Mechanical Engineering, McGill University, 1996.
[13] S. Sarkar, "Dynamic modeling of an articulated forestry machine for simulation and control," MSc. thesis, Department of Mechanical Engineering, McGill University, Canada, 1996.
[14] R. G. Blackburn and J. Sheare, *Fluid Power Control*. Technology Press of M.I.T and John Wiley Publishers, 1960.
[15] H. E. Merritt, *Hydraulic Control Systems*. Wiley and Sons Publishers, Newyork, 1967.
[16] D. McCloy and H. R. Martin, *Control of Fluid Power: Analysis and Design*. Ellis Horwood Publishers Limited, England, 2 ed., 1980.
[17] W. Borutzky, "An energetically consistent bond graph model of a double acting hydraulic cylinder," in *Proceedings of European Simulation Multiconference,*, pp. 203–207, 1993.
[18] P. Dransfield and M. K. Teo, "Using Bond graphs in Simulating an Elecro-mechanical System," *Journal of Franklin Institute*, vol. 308, no. 3, pp. 173–184, 1984.
[19] B. W. Bernard, "Predicting the dynamic response of a hydraulic system using power bond graphs," MSc. thesis, Monach University, Melbourne, Australia, 1983.